Thermal and Mechanical Properties of Stretched Recyclable Polyimide Film

Han-Yi Wang,[1] Ta-Jo Liu,[1] Shur-Fen Liu,[2] Jhy-Long Jeng,[2] Chi-En Guan[2]

[1]*Department of Chemical Engineering, National Tsing Hua University, Hsinchu, Taiwan 300, Republic of China*
[2]*Material and Chemical Research Laboratories, Industrial Technology and Research Institute, Hsinchu, Taiwan 300, Republic of China*

Received 17 September 2010; accepted 10 January 2011
DOI 10.1002/app.34139
Published online 20 April 2011 in Wiley Online Library (wileyonlinelibrary.com).

ABSTRACT: An operating window, which is bounded by two temperatures and draw ratios, defines the stable and defect-free stretching region of a polymer film. Physical properties including the coefficient of thermal expansion (CTE), birefringence, and Young's modulus of a recyclable polyimide (PIR) film were measured under stretching conditions. While values of birefringence and Young's modulus increased with increasing stretching stress in the machine direction, the CTE was found to decrease. A semiempirical model for the prediction of birefringence and Young's modulus under stretching conditions was developed, from which the CTE could be estimated from the Young's modulus data. Theoretically evaluated physical properties were found to be in qualitative agreement with the experimental data. © 2011 Wiley Periodicals, Inc. J Appl Polym Sci 122: 210–219, 2011

Key words: polyimide; uni-axial stretching; birefringence; Young's modulus; coefficient of thermal expansion

INTRODUCTION

Polyimide (PI) has been extensively applied in optical-electronic and other industries, owing to its superior thermal and mechanical properties. In recent years, the use of recyclable polyimide has received wide attention because of environmental considerations.[1,2] PIR is first produced in solution form by first adding soft segments or side chains of different materials to the main chain, to make it soluble in certain solvents such as *N*-methyl-2-pyrrolidone (NMP) or dimethylacetamide (DMAC). The solution is then coated on substrates at room temperature, and the PIR film is produced after drying. The PIR film produced can also be laminated with other materials. The addition of soft segments or side chains such as long alkyl chains onto the PI main chain or alkyl side chains onto the phenylene rings of the PI chain will inevitably change the thermal and mechanical properties of the product.[3–5] For example, the PIR tends to have a higher value of the coefficient of thermal expansion (CTE). This could lead to de-lamination or curling between the PIR films and substrates such as copper foils. A conventional approach to reduce the CTE of PI materials is surface modification by introducing hard segment molecules; for example, biphenyltetracarboxylic acid or benzene rings can be fused at *para*-positions into the main chains. The addition of inorganic nano-particles into the PI material is another approach.[6] Physical methods such as sand blasting or flame, corona and UV rays' treatments were also considered by various researchers.[6–15] However, the main disadvantage of using the above approaches is that the resulting PI materials are in general brittle, which will be more difficult for processing.[8,16–18]

A conventional way of improving the mechanical properties of polymer films is by stretching. A polymer film can be uni-axially or bi-axially stretched to change the orientations of molecules. Most research efforts have been focusing on uni-axial stretching, as it is harder to perform the experiments on bi-axial stretching. Some experimental results were reported on the CTE of certain polymers,[19,20] but the theoretical analyses are very limited in open literature. Sato et al.[21] made an attempt to simulate the molecular orientation, including its relaxation, during the stretching of cycloolefin copolymer films. Hibi et al.[22] proposed an ideal aggregation model to predict the birefringence and Young's modulus of unplasticized poly(vinyl chloride) (PVC). To date, there appears to be no theoretical prediction of physical properties of stretching PI film in the literature.

Several researchers have presented experimental observations on the effect of stretching on physical properties of various polymers other than PI.

Correspondence to: T.-J. Liu (tjliu@che.nthu.edu.tw).
Contract grant sponsor: National Science Council ROC; contract grant number: NSC 95-2221-E-007-132-MT3
Contract grant sponsors: Material and Chemical Lab; Industrial Technology and Research Institute.

Pietralla and Kilian[23] analyzed the variations of birefringence of stretched polyethylene films. Engeln et al.[24] reported the effects of stretching on CTE, Young's modulus, and birefringence of poly(tetrafluoroethylene). Cakmak and Simhambhatla[25] examined the surface roughness during the stretching of poly(etheretherketone) film. Cakmak and Kim[26] analyzed the molecular mechanism of necking for poly(etheretherketone) film, as well as the effects of polymer blend ratio on the maximum molecular arrangement. Kokturk et al.[27] studied the effects of molecular structure and operating temperature on the film surface and the crystallization behavior of polylactic acid. El-Tonsy et al.[28] examined the variation of CTE and the necking phenomenon of polypropylene during stretching. Zhou and Cakmak[29] showed that by introducing polymethylmethacrylate (PMMA) into polyvinylidine fluoride (PVDF), rapid crystallization could be avoided during film stretching, thus minimizing the surface roughness.

Numata and Miwa[30] analyzed the effects of rigid and flexible molecular chains during the stretching of PI films and found that CTE is higher for rigid molecular chains in the stretching direction. Pottiger et al.[31] and Hardaker and Samuels[32] examined PI films of different structures during uni-axial stretching. They discovered that PI film thickness would influence the mechanical properties of PI films. Hinkley et al.[33] investigated the effect of temperature and process variables on modulus, failure strain, and tensile strength of the stretched PI films. Several PI materials were identified as candidates for further property optimization. Hawkins et al.[34] analyzed the stretch-orientation of a special PI film. King et al.[35,36] studied the optical properties of uniaxially stretched PI films. A linear relationship was found between the optical properties and the stretching force before necking appeared. Most of the literature available on the properties of PI is for virgin PI films.

To meet the environmental requirements, the use of PIR film to replace the virgin PI for industrial applications has recently received wider attention. For the ease of processing, it is important that the thermal and mechanical properties of PIR are compatible with the virgin PI. In this study, the stretching experiments are carried out for a PIR to establish an operating window. The window is bounded by temperatures and draw ratios, and stable stretching is possible for a fixed temperature and draw ratio inside the operating window. Optical and physical properties of the stretched film including birefringence, Young's modulus, and CTE are measured. In addition, theoretical works applicable to PI films for the estimations of birefringence and Young's modulus for a given set of temperature and draw ratio inside the operating window are presented. CTE can be evaluated indirectly from a master curve constructed from the existing data of CTE as a function of Young's modulus for different materials[37] and different types of PI.

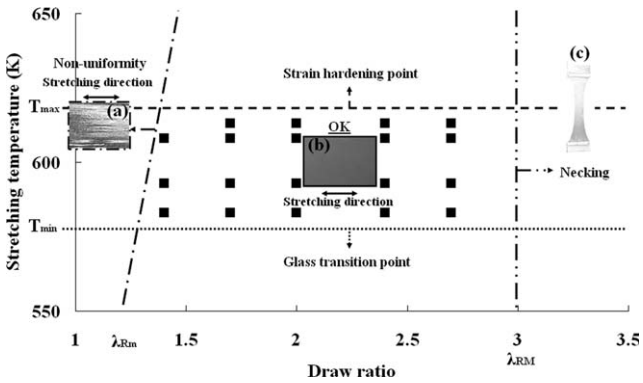

Figure 1 The operating window with temperature and draw ratio as two variables. Square symbols are data points for stretching test.

THEORETICAL

To date, no attempt has been made to predict the CTE of a PI film directly from the uni-axial stretching data.[33–36] In this study, a convenient method to evaluate the CTE is developed. This method requires two sets of experimental data in conjunction with some existing formulas available in the literature. The first set of data is the operating window where the two key variables are the draw ratio λ and the temperature T, λ is defined as the ratio of the stretched film length to the original film length. The experimental data obtained for the PIR film is shown in Figure 1. The operating window is bounded by two temperatures appearing on the ordinate axis where the lower bound $T_{\min}$ is the glass transition temperature, and the upper bound $T_{\max}$ is the strain hardening temperature. The abscissa axis is bounded between a minimum draw ratio λ_{RM}, in which irregular surfaces with streaks would appear and a maximum draw ratio is λ_{Rm}, beyond which necking would appear. The development of the operating window is further discussed in next section.

For a given set of draw ratio λ and temperature T inside the operating window in Figure 1, the birefringence Δn and the optical elastic coefficient C can be obtained with the following formulas[38–40]:

$$\Delta n = \frac{\Delta n_0}{2}\left[\frac{3}{1-\lambda^{-3}} - \frac{3\lambda^{-3/2}\cos^{-1}\lambda^{-3/2}}{\left(1-\lambda^{-3}\right)^{3/2}} - 1\right] \quad (1)$$

$$C = \frac{2\pi\Delta\alpha}{45}\frac{\left(n_{av}^2+2\right)^2}{n_{av}kT} \quad (2)$$

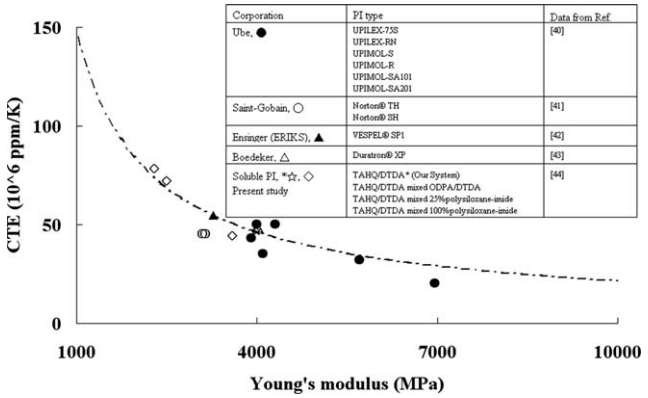

Figure 2 CTE as a function of Young's modulus. Data points were taken from open literature and the present study.

The above information enables the determination of the stretching stress $\Delta\sigma$ and the orientation factor f from the following formulas[39–41]:

$$\Delta\sigma = \frac{\Delta n}{C} \tag{3}$$

$$f = \frac{\Delta n}{\Delta n_0} \tag{4}$$

Once f is available, the Young's modulus E_m in the stretching direction (MD) can be obtained from the following formula[42]:

$$f = 1 - \frac{E_u}{E_m} \tag{5}$$

where E_u is the Young's modulus of the un-oriented polymer, which can be determined from virgin (non-stretching) PI samples.

The Young's modulus E_t in the transverse direction (TD) can also be evaluated with[42]

$$\frac{3}{E_u} = \frac{1}{E_m} + \frac{2}{E_t} \tag{6}$$

To date, there is no theoretical formula relating the Young modulus to the CTE of a polymeric material. However, there were some experimental data presented for various polymers such as acrylonitrile butadiene styrene (ABS), polycarbonate (PC), and others[37] in the form of CTE as a function of Young's modulus. This is the second set of data required for the present approach, as displayed in Figure 2. Figure 2 presents the literature data for different types of polyimides,[43–46] as well as the PI films used in the present study, plotted in the form of CTE versus Young's modulus. It appears that there is a correlation between CTE and the Young modulus, and a master curve can be constructed by a least-square fitting procedure. This curve can be used to determine the CTE from the Young's modulus of a PI sample. When E_m and E_t are available, values of CTE in the stretching and transverse directions, MD and TD, can be evaluated with the aid of Figure 2.[37]

The advantage of the proposed approach is that once an operating temperature is fixed, and a suitable draw ratio is selected, the related stress can be readily obtained using the formulas presented above. Consequently, values of birefringence, Young's modulus, and CTE can be evaluated without experimentation.

EXPERIMENTAL

The procedure for preparing the PIR was described previously by Wang et al.,[47] which was based on a patented formulation.[48] The polymerization was carried out in one-step chemical imidization. Bis(trimellitic acid anhydride)phenyl ester 45.8 g (0.1 mol), 1-(4-aminophenoxy)-4-(4-aminophenyl)-2,6-di-*tert*-butyl-benzene 38.8 g (0.1 mol), and NMP(270 g)/xylene(68 g) cosolvent were mixed at a temperature 273–277 K for about 4 h in a nitrogen environment. The mixture was then heated to 453–473 K, and subjected to dehydration reaction at that temperature for 3 h. The PIR obtained has an intrinsic viscosity of 0.8 dL g^{-1} (NMP, 0.5 dL g^{-1}, 303 K), and a molecular weight between 30,000 and 40,000 g mol^{-1} (MW). The glass transition temperature is around 578 K, and its specific gravity is 1.4. The PIR was dissolved in *N*-methyl-2-Pyrrolidone (NMP), with an initial solid content of 14.6 wt %. The viscosity of the PIR solution was around 5000 mPas. For the stretching experiments, the PIR solution had to be hand-coated on a flat steel plate, then peeled and dried. The detailed procedures: for the film preparation are as follows:

1. A highly polished steel plate with surface roughness less than 1 μm was first cleaned using a nitrogen spray gun to remove dusts, then wiped by acetone. The plate was then immersed into an ultrasonic DI water bath (DC300H, Delta) for 20 min. The plate was wiped by paper and then cleaned again with the nitrogen spray gun.
2. The PIR solution was placed in a mixer (ARE-250, YSC) with steady stirring and de-gassing for 20 min. The solution was then coated on the steel plate by a laboratory blade coating system.
3. The steel plate with the coated film was placed in an oven for drying. The drying temperature was set at 393 K and the drying time was around 500 s.
4. According to the peeling window found by Wang et al.,[47] the PIR film could be peeled

successfully if the solvent concentration of the PIR was between 6.5 and 16.5 wt %. In the present study, the solvent concentration of PIR samples was selected to be 12 wt %.

5. A sharp steel knife was used to cut the coated PIR film into many stripes, each having a width of around 1 cm. One end of the sample was removed from the steel plate, and the stripe was peeled with a Shimadzu machine (AG-5000A, Shimadzu). The peeling speed was fixed at 500 mm min^{-1}. After peeling, each PIR film stripe was cut into rectangular pieces of size 1 cm $\times$ 2 cm for further drying.
6. The PIR samples were placed in a vacuum dryer. The drying temperature was set at 473 K for the first 2 h, and then raised to 523 K for another 2 h. The samples were completely dried and then removed from the oven after 4 h.
7. The residual solvent concentration of the PIR samples was measured with a thermogravimetry analysis (TGA7, Perkin–Elmer), following the procedure of Wang et al.[47] The solvent concentration was found to be less than 0.5 wt % for all the samples.

Before carrying out the stretching experiments, the range of operating temperature that is suitable for stretching had to be established first. This range should be between the glass transition and the strain hardening temperatures. It has been reported[20] that when the stretching temperature is below the glass transition temperature of the material, the material is still in its glassy state and a large stress is required to stretch the film. This could cause slippage between the holding device and the film being stretched. On the other hand, if the stretching temperature exceeds the strain hardening temperature of the material, the material structure is too strong for it to be stretchable.

A dynamic mechanical analyzer (Q800, TA) was needed to perform the film stretching test. The PIR sample was placed under a fixed stretching temperature for 1 h, so that residual stress remained in the film could be totally relaxed. A stretching stress, as calculated from eq. (3), was set and a creep mode was selected to stretch the film until the film reached the specified draw ratio. The sample was then removed from the sample holder and quenched rapidly at room temperature to prevent further molecular relaxation. The final molecular orientation of the sample should be as close as possible to the condition just at the end of stretching.

Several mechanical and optical properties of the stretched samples were measured. A film thickness detector (ID-C112MB, Mitutoyo) was used to measure the film thickness. Following the suggestion of Cakmak and Simhambhatla,[25] the average film thickness was obtained by averaging 10 thicknesses taken at MD position and 10 at TD position. The thickness variation in both MD and TD locations can be presented by a parameter δ, which is defined as

$$\delta \equiv \frac{S_t}{t_{ave}} = \frac{\sum_{i=1}^{N} (h_i - t_{ave})}{t_{ave}\sqrt{N-1}} \tag{7}$$

Here, S_t is the standard deviation of film thickness, t_{ave} is the average film thickness at every draw ratio, h_i is the film thickness at different positions on the same PIR film, and N is the number of positions on the same PIR film.

Birefringence of a polymer is defined as $\Delta n = \bar{n}_x - \bar{n}_y$, where $\bar{n}_x$ and $\bar{n}_y$ are the principal values of the ellipsoids in the x and y directions, respectively. Values of birefringence at three locations of the PIR film were measured using a birefringence analyzer (21ADH, Kobra). The average of these three values was taken as the birefringence of the sample.

$$\Delta n_0 = \frac{2\pi}{9}\frac{(n_{av}^2+2)^2}{n_{av}}\frac{\Delta\alpha}{V_{int}} \tag{8}$$

$$V_{int} = \frac{M}{\rho N_A} \tag{9}$$

According to Ando et al.,[41,49] as the molecular weight of polymer increases, birefringence would be more significant. The effect of coating thickness was not included in the theoretical model developed here. Values of the average refractive index were needed before examining the birefringence of a polymer. The average refractive index is defined as $n_{av} \equiv \frac{(\bar{n}_x+\bar{n}_y+\bar{n}_z)}{3}$, where $\bar{n}_z$ is the principal value of the ellipsoids in the thickness direction. The refractive index was measured by using a prism coupler (SPA-4000, Sairon). As suggested by Coburn et al.,[50] a Shimadzu machine (AG-5000A) was used to measure the Young modulus of the stretched film, with the environmental condition set at 296 K, and 50% RH. The film was stretched at a steady rate of 5.04 mm min^{-1}. The Young's modulus was taken as the slope of the stress–strain curve.

Values of CTE of the PIR samples were determined by a thermal mechanical analyzer (Q400, TA). The measurement was conducted initially at room temperature and then the temperature was raised at a rate 5 K min^{-1} from 298 to 623 K. The CTE was taken as the slope of the dimension change for temperature between 298 and 473 K, which is the appropriate range for industrial applications of various PI films. Following the work of El-Tonsy et al.,[28]

TABLE I
Numerical Values of Parameters for the Theoretical Models

Maximum draw ratio $\lambda_{RM} = 3$	Minimum draw ratio $\lambda_{RM} = 1.2$
Young's modulus of the un-oriented polymer $E_u = 4000$ MPa	Number of positions of the PI film $N = 10$
Average refractive index $T_{max} = 1.63$	Intrinsic birefringence $T_{min} = 0.0077$
Strain hardening temperature $T_{max} = 620$ K	Glass transition temperature $T_{min} = 575$ K
Polarizability anisotropy $\Delta\alpha = 2.96 \times 10^{-29}$ m^3	

images of the molecular orientation at the mid-neck section and the two ends of the PIR film samples were taken using a polarized optical microscopy (POM) (BX51, Olympus).

RESULTS AND DISCUSSION

Values of parameters required for the theoretical calculations are listed in Table I. All the parameters were determined experimentally. The average film thickness is about 18 μm. In carrying out the stretching experiments, a temperature range suitable for stretching must be decided first. Observations on the variation of Young's modulus as a function of temperature can serve as an indicator to determine the operable temperature range.[20] Values of Young's modulus obtained for various PIR samples as a function of temperature are displayed in Figure 3. It is observed that Young's modulus is independent of temperature in the low temperature range up to $T =$ 573 K. The Young modulus then drops sharply as the temperature rises from 573 to 613 K. It reaches a minimum at around 613 K, and increases again with further increase in temperature. According to Shirouzu et al.,[20] a sharp drop of Young's modulus in the temperature range between 573 and 613 K indicates a structural change from the glassy to rubbery state, where the strength of the structure is weakened. When the temperature exceeds 613 K, strain hardening is likely to appear and the strength of PIR is enhanced. It is easier to carry out stretching experiment in the temperature range between 573 and 613 K because the stress required to stretch the sample is smaller, thus preventing the slippage between the PIR film and the holder. Hence, the two operating temperatures selected for the stretching experiment in the present study were 583 and 608 K.

Another critical parameter for the stretching experiment is the draw ratio. The PIR film thickness may become nonuniform during stretching. The nonuniformity can be either in the machine direction (MD) or the transverse direction (TD). The variation of film thickness δ obtained as a function of draw ratio is presented in Figure 4. It is observed that the PIR films are not uniform in TD if the draw ratio is smaller than 1.4. Increasing the stretching stress can minimize the nonuniformity of the film. According to Galay and Cakmak,[51] the surface smoothness is determined by the molecular structure of the film. If the structure is strong, then the resulting surface is smooth; and if the structure is weak, then nonuniform surface will appear during stretching. Higher stretching temperature will reduce the strength of the molecular structure and consequently increases the possibility of surface nonuniformities. The film surface can be smoothened by increasing the draw ratio, owing to the higher stretching stress.

King et al.[35,36] observed the appearance of necking when the draw ratio was too high. Necking implies a variation of physical properties of the test sample due to the unevenness of molecular orientation. However, necking cannot be easily identified by just observing the appearance of samples. Photographs of the PIR samples taken at two temperatures and different draw ratios are shown in Figure 5. Even though the widths of the PIR samples are smaller in

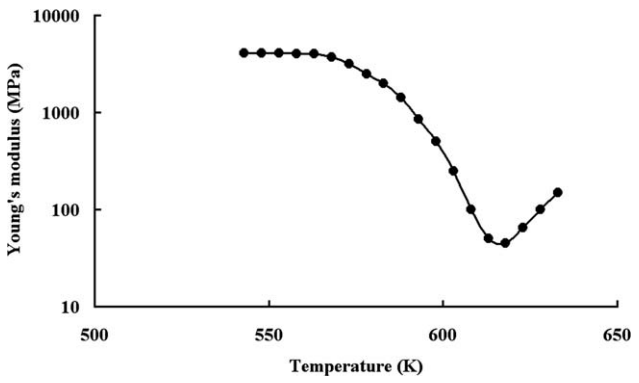

Figure 3 Young's modulus as a function of temperature for PIR samples.

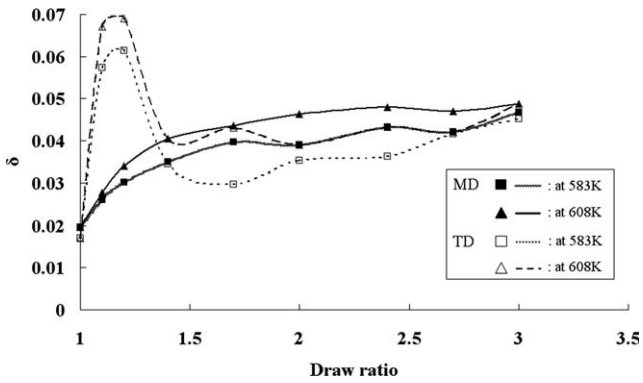

Figure 4 Variations of thickness of PIR film samples in both MD and TD at two temperatures.

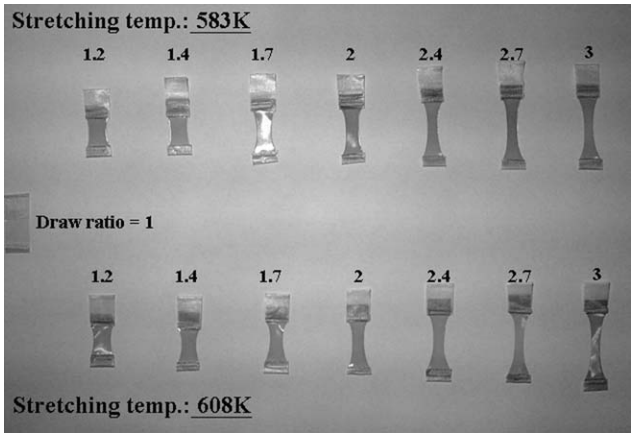

Figure 5 Photos of samples at different draw ratios and temperatures.

the middle section at high draw ratio, there is no guarantee that necking exists simply from its appearance. King et al.[35,36] proposed that necking could be evaluated by examining the birefringence of the stretched samples. El-Tonsy et al.[28] suggested that necking could also be observed at the mid-neck and the two down-neck points by polarized optical microscopy. In the present study, birefringence data were taken at three points in each sample: one in the

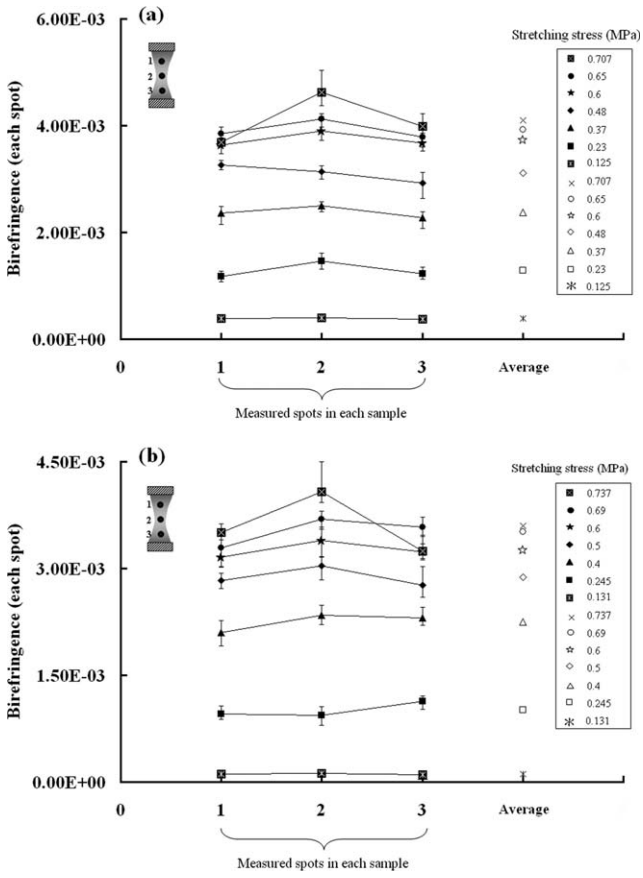

Figure 6 Values of birefringence at three points and the average of each sample.

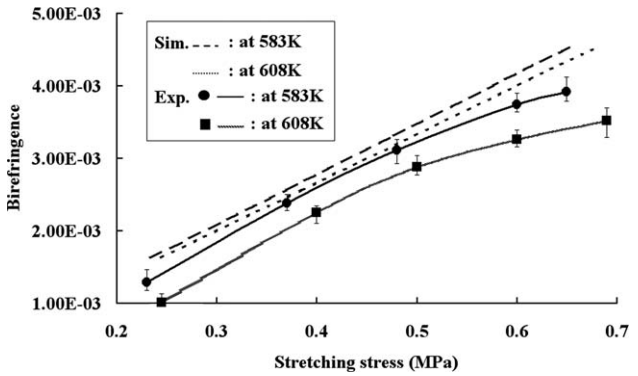

Figure 7 Comparison of theoretically predicted birefringence with experimental data of PIR samples at two temperatures.

middle section and two close to the two end sections. Figure 6 presents values of birefringence of each sample measured at three specific locations, as denoted as 1, 2, and 3 on the abscissa axis and the average value. Values of the stress at different draw ratios were computed using eq. (1). It was found that at draw ratio $\lambda = 3$, the variation of birefringence between the two experimental temperatures appears to be the largest. Hence, this is considered as the maximum draw ratio for necking. Above the maximum draw ratio, necking becomes significant and no uniform physical properties could be obtained. A film is considered to be uniform film when the standard deviation divided by the mean thickness is less than 5%.[51] The data shown in Figure 4 indicate that films are uniform at two temperatures 583 and 608 K when the draw ratio is between 1.4 and 3. On the basis of the above analysis, an operating window for film stretching the window, bounded by temperature and draw ratio, is presented in Figure 1. The operable temperature range is between the glass transition point and the strain hardening point. The thickness of the sample will be non-uniform when the draw ratio is too low, and necking will appear when the draw ratio is too high. Comparison of the theoretical predictions of birefringence, Young's modulus and CTE of PIR samples with the experimental results were carried out at temperatures and draw ratios inside the operating window, as indicated by the square symbols in Figure 1.

Comparison of the theoretically predicted values of birefringence with the experimental results is displayed at Figure 7. Data were based on five draw ratios from 1.4 to 3.0 at two temperatures. It is seen that birefringence increases with increasing stretching stress increases at both temperatures. At the same stretching stress, higher temperature yields a lower value of birefringence, owing to the relaxation of stretching molecules at higher temperature. The theoretical predictions are higher than the experimental

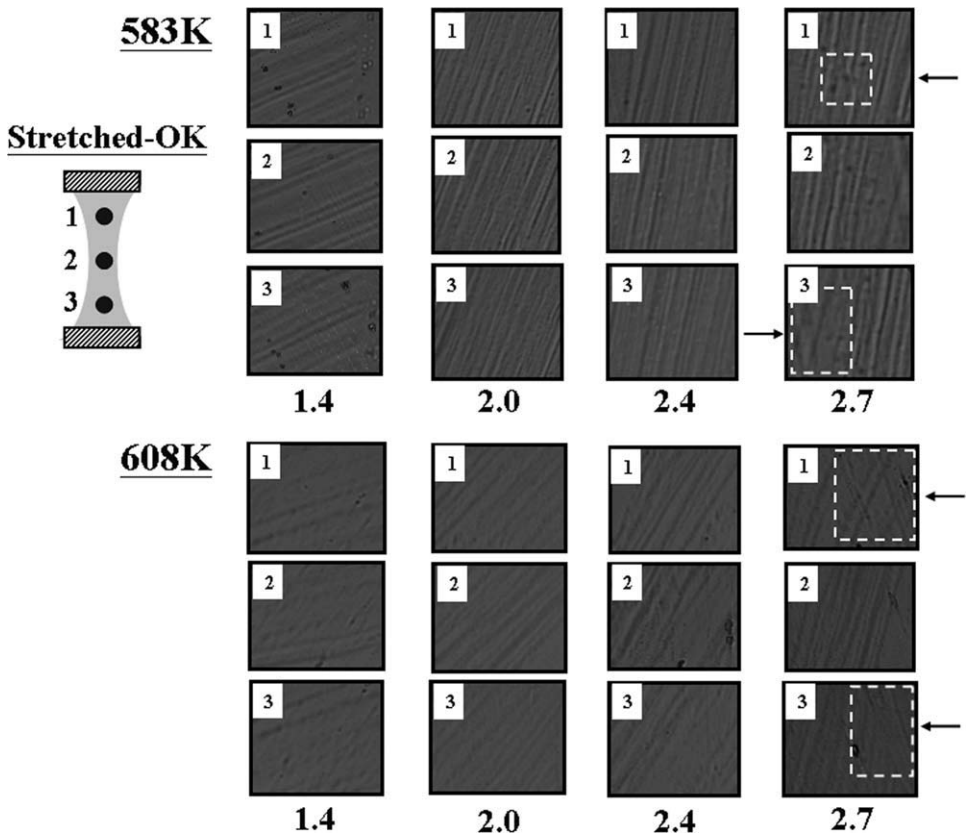

Figure 8 POM images at three locations of PIR samples at different draw ratios. Arrows mark the areas with higher irregular patterns of molecular orientations.

observations for both temperature and stretching stress ranges. The discrepancies appear to be more significant at high stretching stress. This observation was further examined from the polarized optical microscopic images (POM), which show the molecular orientation patterns of samples at different draw ratios between 1.4 and 2.7, and temperatures 583 and 608 K, as shown in Figure 8. El-Tonsy et al.[28] observed a fibril structure of the stretched poly(propylene) sample at the mid-point of the sample at lower λ, and the structure was less regular at two end points of the sample. The images in Figure 8 show a similar pattern. Regular fibril structure was observed when λ is less than 2.4. At $\lambda = 2.7$, irregular patterns shown inside the dotted enclosure as marked by arrows were observed at two end points. When the draw ratio is above 2.4, molecules at the mid-neck section in the stretched PI film are regularly oriented, but not at the two ends. The model developed here was based on the assumption that molecular orientation would not be influenced by imminent necking. Hence, the prediction may not be correct if necking affects the molecular orientation. Therefore the deviations between the predictions and the experimental results are larger at high draw ratios.

Comparison of the theoretical predictions of Young's modulus E_m in the MD direction with the experimental results is displayed in Figure 9. The trend is similar to the birefringence results shown in Figure 7, i.e., the Young modulus increases with increasing stretching stress due to the molecular anisotropy in the stretching direction. For the same stretching stress, E_m is smaller at higher stretching temperature, because the sample becomes more isotropic. The differences of E_m between the two temperatures are less significant at lower stress. The theoretically predicted values of E_m are higher than the experimental values, with a maximum deviation of about 10%, occurring at the draw ratio 2.7.

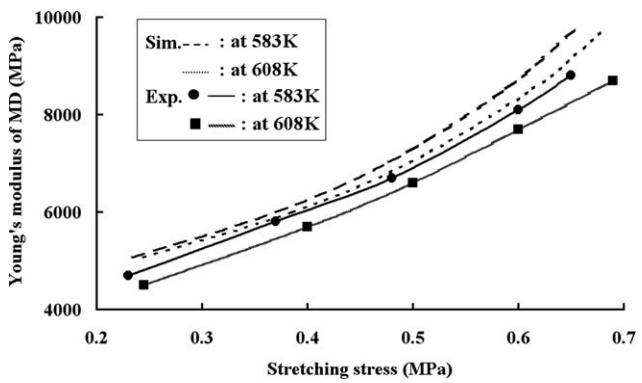

Figure 9 Comparison of theoretically predicted Young's modulus in MD with the experimental data at two temperatures.

Pottiger et al.[31] found that there exists a linear relationship between Young's modulus and stretching stress for polyimide films. This appears to be not the case from the present findings. It should be pointed out, however, that the observation of Pottiger et al.[31] was based on draw ratios less than 2. At higher draw ratios, the linear relationship may no longer exist owing to the increasing nonuniformity of molecular orientations at two ends of the stretched PIR samples, as shown in Figure 8.

Figure 10 compares the predictions of CTE in the machine direction (MD) and the experimental results. Both theory and experiment indicate that stretching can effectively reduce the CTE of the PIR films. CTE is an indicator on the deformation resistibility of the material during the temperature ramp. Values of CTE become smaller as the stretching stress goes up because the molecular orientations of PIR samples become more and more anisotropic and enhance the deformation resistibility. In contrast to the birefringence and Young's modulus, the predicted CTE values are lower than the experimental results throughout the whole range of stretching stresses. This is due to the fact that the model assumes molecules are arranged in perfect order, which is not valid especially in the higher stress region. In addition, although the effect of temperature on CTE appears to be insignificant from the prediction, the experimental CTE drops markedly over a 20° drop in the stretching temperature. The experimental results indicate the importance of temperature because of the relaxation behavior of PIR molecules during stretching.

Theoretical predictions of Young's modulus and CTE in the transverse direction (TD) as a function of stretching stress are displayed in Figure 11. Owing to the narrow width (less than 1 cm) of the PIR samples prepared, it was difficult to carry out experimental measurements of Young's modulus and CTE. The theory predicts that an increasing Young's modulus and decreasing CTE as the stretching stress increases.

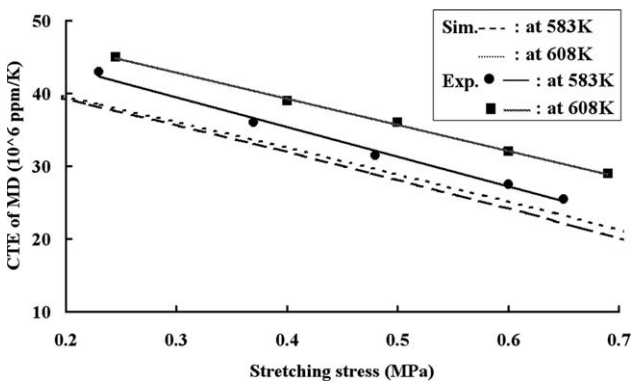

Figure 10 Comparison of theoretically predicted CTE in MD with the experimental data at two temperatures.

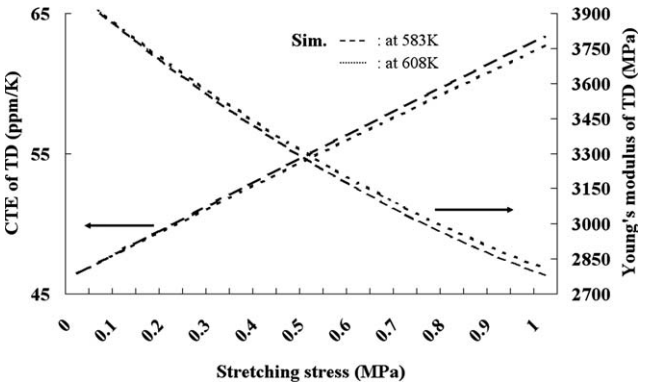

Figure 11 Theoretically predicted Young's modulus and CTE of PIR samples in TD at two temperatures.

The aggregation model of Hibi et al.[22] can be used to predict the physical properties such as birefringence and Young's modulus of PI film, but it does not include the temperature effect. Shirouzu et al.[20] and Engeln et al.[24] pointed out that stretching temperature could be important as it influences the molecular orientations and the physical properties of the polymer. Since the theoretical model presented here neglects the relaxation behavior during stretching, consequently the predicted effects of temperature on both Young's modulus and CTE in the both MD and TD are not significant.

CONCLUSIONS

The effects of applying uni-axial stretching to control and reduce the coefficient of thermal expansion for a recyclable film were examined in the present study. An operating window, bounded by two limiting temperature and draw ratios, for stable stretching was established experimentally. The two limiting temperatures are the glass transition and the strain hardening temperatures. The two draw ratio bounds are the minimum draw ratio, which marks the onset of rough and nonuniform surface, and the maximum draw ratio, before the appearance of necking.

A PIR film is stretchable without defects for a given set of operating temperatures and draw ratios inside the operating window. Physical properties including CTE, birefringence and Young's modulus were measured under stretching conditions. It was found that both birefringence and Young's modulus in the machine direction of the PIR film increases as the stretching stress increases, but an opposite trend was observed for CTE. The effect of temperature is less significant on these physical properties.

A model for the estimation of the mechanical and thermal properties of PIR film was proposed. The birefringence and Young's modulus can be estimated for a given set of operating temperature and

draw ratio, from which the required stress can be determined. A master curve can be constructed based on the experimental data that relate Young's modulus to CTE for different types of PI materials currently available in open literature. This curve can be used to estimate the CTE of PIR from Young's modulus data.

Comparisons of the theoretical predictions with the experimental data showed that the theory overpredict the birefringence and Young's modulus, but under predicts the CTE at the same stretching temperature and stress. This is due to the fact that the theoretical model does not include the effect of molecular orientation. Although there are certain discrepancies between the theoretical and experimental values, the general trends of variation are similar and qualitative agreement is obtained. Young's modulus and CTE in the transverse direction were difficult to obtain experimentally due to sample size, but they can also be evaluated from the model.

Valuable suggestions of Prof. Carlos Tiu, Monash University, Australia, were highly appreciated.

NOMENCLATURE

Alphabets

C	Optical-elastic coefficient, (2) m N^{-2}
E_m	Young's modulus of stretched PI film in MD, (5) N m^{-2}
E_t	Young's modulus of stretched PI film in TD, (6) N m^{-2}
E_u	Young's modulus of the un-oriented polymer, (5) N m^{-2}
f	Orientation factor, (4)
h_i	The film thickness on different positions of the PI film, (7) m
k	Boltzmann constant, (2) J K^{-1}
M	Molecular weight of polymer, (9) g mol^{-1}
N	Number of positions of the PI film, (7)
N_A	Avogadro's number, (9) mol^{-1}
n_{av}	Average refractive index, (2)
$\overline{n}_x$	Refractive index of the ellipsoids in the film plane
$\overline{n}_y$	Refractive index of the ellipsoids in the film plane
$\overline{n}_z$	Refractive index of the ellipsoids out of the film plane
Δn	Birefringence of polymer film, (1)
Δn_0	Intrinsic birefringence, (1)
S_t	Standard deviation of film thickness, (7) m
T	Stretching temperature, (2) K
T_{max}	Strain hardening temperature, K
T_{min}	Glass transition temperature, K
t_{ave}	Average film thickness at every draw ratio, (7) m
V_{int}	Intrinsic volume of repeating unit, (8) m^3

Greek letters

$\Delta\alpha$	Polarizability anisotropy, (2) m^3
δ	Parameter of thickness variation, (7)
λ	Draw ratio, (1)
λ_{RM}	Maximum draw ratio
λ_{Rm}	Minimum draw ratio
ρ	The density of polymer, (9) kg m^{-3}
$\Delta\sigma$	Stretching stress,(3) N m^{-2}

References

1. Ghosh, M. K.; Mittal, K. L.; Polyimides: Fundamentals and Applications; Marcel Dekker: New York, 1996.
2. Wilson, D.; Stenzenberger, H. D.; Hergenrother, P. M. Polyimides; Chapman and Hall: New York, 1990.
3. Rabilloud, G.; Senneron, M.; Cohen, C.; Mariaggi, P.; Sillion, B. US Patent 4,736,015, 1988.
4. Yin, J.; Ye, Y. F.; Wang, Z. G. Eur Polym Mater 1998, 34, 1839.
5. Wang, D. H.; Shen, Z.; Guo, M.; Cheng, S. Z. D.; Harris, F. W. Macromolecules 2007, 40, 889.
6. Tang, J. C.; Lin, G. L.; Yang, H. C.; Jiang, G. J.; Chen-Yang, Y. W. J Appl Polym Sci 2007, 104, 4096.
7. Okahashi, M.; Tsukuda, A.; Miwa, T.; Edman, J. R.; Paulson, C. M., Jr. US Patent 5,324,475, 1994.
8. Okahashi, M.; Tsukuda, A.; Miwa, T.; Edman, J. R.; Paulson, C. M., Jr. US Patent 5,460,890, 1995.
9. Yamamoto, T.; Hosoma, T.; Yoshioka, K. US Patent 6,251,507 B1, 2001.
10. Fujihara, K.; Ono, K.; Matsuwaki, T. US Patent 0,042,167 A1, 2007.
11. Yamaguchi, H.; Murakami, M.; Kohda, M. US Patent 0,044,681 A1, 2008.
12. Nagano, H.; Kawai, H.; Nojiri, H.; Yamamoto, T. US Patent 4,742,099, 1988.
13. Chan, K. P.; Hagberg, E.; Mullen, T. J.; Odle, R. R. US Patent 0,044,639, 2008.
14. Auman, B. C. US Patent 5,260,408, 1993.
15. George, D. E. US Patent 5,284,904, 1994.
16. Hamamoto, T.; Inoue, H.; Miwa, Y.; Hirano, T.; Imatani, K.; Matsubara, K.; Kohno, T. US Patent 5,308,569, 1994.
17. Yabuta, K.; Akahori, K. US Patent 0,074,686 A1, 2002.
18. Asakura, T.; Mizouchi, M.; Kobayashi, H. US Patent 4,470,944, 1984.
19. Fay, C. C.; Stoakley, D. M.; St Clair, A. K. High Perform Polym 1999, 11, 145.
20. Shirouzu, S.; Ishii, T.; Iga, T.; Chino, S.; Hayashi, M.; Tomioka, T.; Sibasaki, S.; Arai, Y.; Ooki, Y.; Hayashi, K. Jpn J Appl Phys Part 1 (Regular Papers and Short Notes and Review Papers) 1995, 34, 4880.
21. Sato, T.; Itadani, M.; Arakawa, K.; Yamada, T. Jpn J Appl Phys 2007, 46, 7782.
22. Hibi, S.; Maeda, M.; Kubota, H. Polymer 1977, 18, 801.
23. Pietralla, M.; Kilian, H. G. J Polym Sci Polym Phys Ed 1980, 18, 285.
24. Engeln, I.; Hengl, R.; Hinrichsen, G. Colloid Polym Sci 1984, 262, 780.

25. Cakmak, M.; Simhambhatla, M. Polym Eng Sci 1995, 35, 1562.
26. Cakmak M.; Kim, J. C. J Appl Polym Sci 1997, 65, 2095.
27. Kokturk, G.; Serhatkulu, T. F.; Cakmak, M.; Piskin, E. Polym Eng Sci 2002, 42, 1619.
28. El-Tonsy, M. M.; Meikhail, M. S.; Felfel, R. M. J Appl Polym Sci 2006, 100, 4452.
29. Zhou, X.; Cakmak, M. Polym Eng Sci 2007, 47, 2110.
30. Numata, S.; Miwa, T. Polymer 1989, 30, 1170.
31. Pottiger, M. T.; Coburn, J. C.; Edman, J. R. J Polym Sci Part B Polym Phys 1994, 32, 825.
32. Hardaker, S. S.; Samuels, R. J. J Polym Sci Part B Polym Phys 1997, 35, 777.
33. Hinkley, J. A.; Dezern, J. F.; Feuz, L.; Klinedinst, D. Polym Eng Sci 2004, 44, 1360.
34. Hawkins, B. P.; Hinkley, J. A.; Moore, J. High Perform Polym 2006, 18, 469.
35. King, J. S.; Whang, W. T.; Lee, W. C.; Chang, L. M. Jpn J Appl Phys 2006, 45, L501.
36. King, J. S.; Whang, W. T.; Lee, W. C.; Chang, L. M. Mater Chem Phys 2007, 103, 35.
37. Erhand, G.; Designing with Plastics; Hanser: Cincinnati, 2006.
38. Tanaka, M.; Young, R. J. Macromolecules 2006, 39, 3312.
39. Van der Heijden, P. C.; de la Rosa, A.; Gebel, G.; Diat, O. Polym Adv Technol 2005, 16, 102.
40. Van Krevelen, D. W. Properties of Polymers, 3rd ed.; Elsevier: New York, 1990.
41. Ando, S.; Sawada, T.; Sasaki, S. Polym Adv Technol 2001, 12, 319.
42. Nielsen, L. E.; Landel, R. F. Mechanical Properties of Polymers and Composites, 2nd ed.; Marcel Dekker: New York, 1994.
43. Heltzel, S.; Semprimoschnig, C. O. A. High Perform Polym 2004, 16, 235.
44. Young, I. Chem Week 1999, 161, 22.
45. Murari, A.; Vinante, C.; Monari, M. Vacuum 2002, 65, 137.
46. Swift, G. W.; Packard, R. E. Cryogenics 1979, 19, 362.
47. Wang, H. Y.; Liu, T. J.; Liu, S. F.; Jeng, J. L. Polym Eng Sci 2010, 50, 1128.
48. Chern, Y. T.; Ju, M. H. Macromolecules 2009, 42, 169.
49. Terui, Y.; Ando, S. J Polym Sci Part B Polym Phys 2004, 42, 2354.
50. Coburn, J. C.; Pottiger, M. T.; Noe, S. C.; Sentu-Ria, S. D. J Polym Sci Part B Polym Phys 1994, 32, 1271.
51. Galay, J.; Cakmak, M. J Polym Sci Part B Polym Phys 2001, 39, 1107.